Kinetics of membrane flux decline: the role of natural colloids and mitigation via membrane surface modification

James E. Kilduff[1], Supatpong Mattaraj[2], Mingyan Zhou[1] and Georges Belfort[3]
[1]*Department of Civil and Environmental Engineering, Rensselaer Polytechnic Institute, 110, 8th Street, Troy, NY 12180, USA (Tel.: +1-518-2762042; Fax: +1-518-2762095; E-mail: kilduff@rpi.edu); [2]Faculty of Engineering, Chemical Engineering, Ubon Ratchathani University, Ubon Ratchathani 34190, Thailand; [3]Isermann Department of Chemical Engineering, Rensselaer Polytechnic Institute, 110, 8th Street/210A Rickets Building, Troy, NY 12180, USA*

Abstract

Applications of membrane technologies for potable water production have been expanding significantly, leading to increased efforts to control membrane fouling, which can significantly reduce membrane performance, increase operating costs, and shorten membrane life. Natural organic matter is ubiquitous in all water supplies and has been implicated as a major contributor to fouling during filtration of natural water. In this review, we discuss factors that influence NOM fouling, including hydrodynamics; properties of the feed constituents such as size, hydrophobicity, charge density and isoelectric point; properties of the membrane including hydrophobicity, charge density, surface roughness, and porosity; and properties of the solution phase such as pH, ionic strength and concentration of metals. We review approaches to identify and mathematically describe fouling kinetics, including effects of pore blockage, cake formation, and osmotic pressure. Finally, we discuss strategies to mitigate fouling, with a focus on strategies that involve a modification of the nanostructure of membrane surfaces, via UV-assisted graft polymerization of hydrophilic monomers to increase surface wettability and reduce interactions between NOM and the membrane surface.

Introduction

Applications of membrane technologies for potable water production have been expanding significantly; a dramatic example of this effort is the construction of the 140,000 m³/d Mery-sur-Oise filtration plant, which serves part of the City of Paris, France. Microfiltration (MF) membranes remove particulates and control turbidity; ultrafiltration (UF) membranes can provide protection from pathogenic microorganisms (including protozoans, bacteria, and viruses) and partially remove natural dissolved organic matter (NOM); and nanofiltration (NF) membranes remove divalent cations (water softening) and can effectively remove NOM. NOM removal is an important strategy to reduce the formation of disinfection by-products, including trihalomethanes and haloacetic acids, which are produced when NOM reacts with chlorine during potable water disinfection. Some disinfection by-products in drinking water are suspected to be toxic, carcinogenic and

mutagenic to humans (Minear & Amy, 1996), and are regulated by the U.S. EPA through the Disinfectants/Disinfection By-products (D/DBP) Rule. The economics of NF processes for NOM removal and disinfection by-product control are becoming increasingly competitive (Blau et al., 1992; Allegeir & Summers, 1995; Visvanathan et al., 1998; Chellam, 2000).

New membrane technology has resulted in materials offering improved water flux, improved salt rejection, and lower operating pressures. However, membrane fouling can significantly reduce membrane performance, increase operating costs, and shorten membrane life (Nilson & DiGiano, 1996). The economical development of water treatment technologies employing membranes requires an understanding of fouling mechanisms and ways to control them. Natural organic matter is ubiquitous in all water supplies and has been implicated as a major contributor to fouling during filtration of natural water. In this review, we will discuss NOM properties that influence fouling, approaches to identify and mathematically describe fouling kinetics, and strategies to mitigate fouling. Our focus will be on mitigation strategies that involve a modification of the nanostructure of membrane surfaces, via UV-assisted graft polymerization.

Natural organic matter

Natural organic matter properties

Naturally occurring dissolved and colloidal organic matter (NOM), acting alone or in concert with inorganic ions and colloids, is considered a major contributor to membrane fouling in water treatment applications, including microfiltration (Kaiya et al., 1996; Yuan & Zydney, 1999a, b), ultrafiltration (Mallevialle et al., 1989; Jucker & Clark, 1994; Cho et al., 1999; Kabsch-Korbutowicz et al., 1999; Lin et al., 1999; Cho et al., 2000a, b; Maartens et al., 2000) and nanofiltration (Nilson & DiGiano, 1996; Hong & Elimelech, 1997; Braghetta et al., 1997, 1998; Alborzfar et al., 1998; Yoon et al., 1998; Combe et al., 1999; Manttari et al., 2000). Natural organic matter is present in all surface and ground waters, with total organic carbon concentrations generally ranging from 1 to 8 mg l^{-1} and median concentrations of 3.4 mg l^{-1} and 0.8 mg l^{-1}

in surface water and ground water, respectively (Symons et al., 1975; Krasner et al., 1995). NOM is a heterogeneous mixture of complex organic materials including humic substances, hydrophilic acids, proteins, lipids, carboxylic acids, amino acids, and hydrocarbons. Humic substances comprise the bulk of organic substances in natural systems; estimates range from 30 to 70% (Thurman, 1985; Buffle, 1990). Carbohydrates and proteinaceous materials may be adsorbed or covalently bonded to a humic substance 'core' (Malcolm, 1990; Shulten & Schnitzer, 1993). The molecular size and weight of humic substances have been estimated using a variety of techniques, and reported weight-averaged molecular weights (M_w) for aquatic humic substances generally range from 1500 to 5000 g mol^{-1} for humic acids and from 600 to 2000 g mol^{-1} for fulvic acids (Thurman et al., 1982; Beckett et al., 1987; Aiken & Malcolm, 1987; Reid et al., 1990; Chin & Gschwend, 1991; Chin et al., 1994). Estimated radii of gyration of humic substances fall in the range of 4.5–30 Å (Thurman et al., 1982; Cameron et al., 1972; Cornel et al., 1986). However, as will be shown, aggregation is possible and can significantly increase NOM size.

NOM isolation

Water from the Tomhannock reservoir in Troy, NY (TMK water), a typical source of NOM in terms of organic carbon content (3 mg l^{-1}), humic content (40%) and molecular weight (1200 Da), was used in much of the research reported in this paper. Reservoir water was first pretreated by microfiltration (using a 0.45-micron cartridge filter) and softened by ion exchange, and then concentrated by reverse osmosis. Previous research has shown that such treatment has little impact on the reactivity of organic matter in terms of nanofiltration membrane fouling, sorption by synthetic resins and activated carbon, and molecular weight distribution measured using size exclusion chromatography (Kilduff et al., 2004a). Natural organic matter passing a 0.45-micron membrane is typically defined as dissolved (DNOM), whereas the retained fraction is considered particulate (PNOM). As a result of the pretreatment employed, the organic matter used in this research is the dissolved fraction of the total organic matter in the Tomhannock reservoir. However, because aggregation and/or precipitation is possible under

filtration conditions, and because organic matter may deposit on membrane surfaces, we will not attempt to make a distinction between particulate and dissolved organic matter during the filtration process, and will refer to the natural organic matter simply as NOM.

Because NOM is a heterogeneous mixture of various organic molecules, its isolation and fractionation into more homogeneous components has been a common approach in characterization and reactivity studies. Adsorption is a widely employed technique to isolate and separate NOM components into operationally defined fractions depending on their affinities to different synthetic resins and their back-elution efficiencies (Leenheer, 1981; Thurman & Malcolm, 1981; Malcolm & McCarthy, 1992; Aiken et al., 1992; Leenheer et al., 2000). Humic components (i.e., 'hydrophobic acids' including humic acids, fulvic acids, and tannins) are isolated by adsorption to XAD-8, a neutral methylmethacrylate resin, at pH 2. More polar species are isolated by adsorption on XAD-4, a styrene-divinyl benzene resin. Species not adsorbed to either XAD-8 or XAD-4 resins are termed hydrophilic, and may include small organic acids, sugars, and perhaps amino acids (Leenheer & Croue, 2003).

Fouling by NOM – Theory and models

Flux decline caused by organic macromolecules (acting alone or in concert with inorganic species, including inorganic colloids) may result from concentration polarization, from pore blockage by solute adsorbed on the membrane surface or within pores, and from the formation of a cake layer on the membrane surface, which presents a resistance to flow in addition to the membrane itself. Concentration polarization effects have been shown to be small in comparison with pore blockage and surface deposition (Cho et al., 1999; Yuan & Zydney, 2000). Based on the complexity of NOM, including the wide distribution of molecular sizes, it is reasonable to expect fouling by both pore blockage and surface deposition, especially when the size distributions of feed solution components and membrane pores exhibit significant overlap.

Dead-end filtration

For dead-end filtration under constant applied pressure, rate laws corresponding to pore blockage, pore constriction, and cake formation can be written by assuming that the number of pores, the pore diameter, or the mass of a cake layer formed at the membrane surface, respectively, change in proportion to the convective transport of mass to the membrane surface. Various fouling models are obtained for each fouling mode (e.g., see Kilduff et al., 2002), which can all be formulated as a single equation as shown by Hermia (1982):

$$\frac{d^2t}{dW^2} = k\left(\frac{dt}{dW}\right)^n, \tag{1}$$

where t is time (s), W is the mass filtered (kg), k is a fouling coefficient with units that depend on the value of n (e.g., $s\ kg^{-2}$, for $n=0$) and n is a dimensionless filtration constant that reflects the mode of fouling: (i) cake formation corresponds to $n=0$; (ii) complete pore blocking corresponds to $n=2$; and, (iii) standard blocking (pore constriction) corresponds to $n=1.5$.

Combined pore blockage cake filtration

Ho and Zydney (2000) developed a model for dead-end filtration (UF and MF) of proteins that combines pore blockage and cake filtration modes of fouling. This model has more recently been applied to filtration of natural organic matter (Kilduff et al., 2002; Taniguchi et al., 2003a). In this model, total flow through the membrane at any time during filtration, Q (kg s^{-1}), is the sum of flow through open pores (through which the resistance is R_m) and through partially blocked pores on which a cake has formed, offering additional resistance to flow. In the absence of significant cross-flow, the combined pore blockage-cake filtration model is written:

$$Q = Q_o\left[\exp\left(-\frac{\alpha_b \Delta P C_f}{R_m}t\right) + \frac{R_m}{R_m + R_c}\right.$$
$$\left. \times \left(1 - \exp\left(-\frac{\alpha_b \Delta P C_f}{R_m}t\right)\right)\right], \tag{2}$$

where α_b is the pore blockage parameter (m^2 kg^{-1} solute); note that bulk or feed concentration, C_f, is in weight fraction units. The resistance from cake

formation, R_c, which increases as a function of time in proportion to the rate that NOM mass accumulates on the membrane surface, is obtained from:

$$\frac{R_m + R_c}{R_m + R_{c,0}} = \sqrt{1 + \frac{2\alpha_c \Delta P C_f}{(R_m + R_{c,0})^2} t},\qquad (3)$$

where α_c (Pa m^4 s kg^{-2}) is the cake formation parameter and $R_{c,o}$ is the initial resistance of the deposit (i.e., a leakage flow). Extensions to systems having significant cross flow were developed by Kilduff et al. (2002). This model is applicable when the resistance caused by concentration polarization is small, i.e., when salt rejection is negligible. The first term in Equation (2) is equivalent to the classical pore blockage model; this term dominates when t is small ($t \ll R_m/\alpha\Delta P C_f$) and the magnitude of the second term becomes negligible. At long times, ($t \gg R_m/\alpha\Delta P C_f$) the second term dominates and the volumetric flux is governed by the classic cake filtration model.

Effects of osmotic pressure

When the feed solution contains both salt and NOM and salt rejection is significant, the effects of concentration polarization cannot be neglected. The change in solution flux is related to the change in osmotic pressure as a result of concentration polarization (assumed to be primarily caused by salt), and the change in the hydraulic resistance of the NOM cake that forms on the membrane surface (Kilduff et al., 2004a). Applied to a well-mixed system with crossflow (e.g., a feed and bleed system with a recycle loop) the rate of flux decline is given by:

$$\frac{dJ_v}{dt} = -\frac{\sigma_s \alpha_s \mathfrak{R}_{mem} \beta_s}{\mu(R_m + R_c)}\left(\frac{dC_{reten,s}}{dt}\right)$$
$$- \frac{J_v}{(R_m + R_c)}\left(\frac{dR_c}{dt}\right)\qquad (4)$$

In Equation (4), the change in osmotic pressure difference across the membrane is expressed in terms of the change in the directly measurable bulk (retentate recycle loop) salt (NaCl) concentration, $C_{reten,s}$. First, the osmotic pressure difference is expressed in terms of the concentration at the membrane surface, C_{mem}, using the definition of intrinsic membrane rejection, $\mathfrak{R}_{mem}$. Then, con-

centration at the membrane surface, C_{mem}, was eliminated in favor of $C_{reten,s}$ by comparing clean water flux (which yields the membrane resistance, R_m) and NaCl solution flux measured under steady-state conditions with different salt concentrations. Data from such experiments were used to calculate osmotic pressure difference, which was related to C_{mem} using a literature correlation (α_s). The ratio $\beta_s = C_{mem}/C_{reten}$, which reflects the degree of concentration polarization, was then computed and correlated as a function of NaCl concentration. The term σ_s is the osmotic reflection coefficient, estimated as the intrinsic membrane resistance, and other terms have been defined previously. In the cake formation model, the time rate of change in cake resistance is assumed to be proportional to the rate of change in cake mass, m_{cake} (kg), which increases at a rate proportional to the net rate of convective mass transport toward the membrane surface:

$$\frac{dR_c}{dt} = \alpha_{cake}\frac{1}{A_m}dm_{cake}\frac{1}{dt}$$
$$= \alpha_{cake}C_{reten,NOM}(t)(J_v - J^*),\qquad (5)$$

where α_{cake} is the specific cake resistance (assumed constant) (m kg^{-1}), $C_{reten,NOM}$ is the NOM concentration in the retentate recycle loop (kg m^{-3}), and J^* (m s^{-1}) is the effective flux associated with back-transport resulting from crossflow. The changes in the bulk salt and NOM concentrations, dC_{reten}/dt, were determined using an overall material balance on the retentate recycle loop, which was shown to approximate a well-mixed condition. Equations (4) and (5) require numerical integration (e.g., Runge-Kutta technique) using the specific cake resistance and the effective back-transport flux (J^*) as calibration parameters.

Factors affecting flux decline during NOM filtration

Factors potentially affecting membrane fouling by NOM include the hydrodynamics of the membrane system, characterized by solution flux and surface shear (Hong & Elimelech, 1997; Cho et al., 1999; Braghetta & DiGiano, 1998); properties of the feed constituents such as size, hydrophobicity, charge density and isoelectric point (Jucker & Clark, 1994; Nilson & DiGiano, 1996; Hong and Elimelech, 1997; Cho et al., 1999, 2000b; Lin

et al., 2000; Carroll et al., 2000); properties of the membrane including hydrophobicity, charge density, surface roughness, and porosity (Combe et al., 1999; Kilduff et al., 2000); and properties of the solution phase such as pH, ionic strength and concentration of metals (Jucker & Clark, 1994; Braghetta & DiGiano, 1997; Hong & Elimelech, 1997; Braghetta & DiGiano, 1998; Yoon et al., 1998; Combe et al., 1999; Yuan & Zydney 1999a; Cho et al., 2000b, Jones & O'Melia, 2000; Lin et al., 2000; Kilduff et al., 2004a).

Effects of fluid shear

Fluid shear at the membrane surface increases with increasing crossflow velocity, enhancing mass transport away from the membrane surface. Figure 1 illustrates the effects of crossflow velocity and recovery ($r = Q_{perm}/Q_{feed}$) on flux decline during nanofiltration of pretreated (microfiltered and softened) Tomhannock Reservoir (TMK) water. As the crossflow velocity increases, increased back-transport reduces the mass transported to the membrane surface by convection, and thus reduces the mass accumulated on the membrane. In terms of the osmotic pressure/cake formation model (Equations (4) and (5)) an increase in back transport is reflected in an increased value of J^*, the effective back-transport flux. This back-transport flux is essentially equivalent to a mass transfer coefficient, k (acting away from the membrane); the rate of flux decline decreases with decreasing values of J_v/k (Cho et al., 1999). When membrane systems are operated at low values of J_v/k, the rate of flux decline becomes small (Hong & Elimelech, 1997; Cho et al., 1999). This can be seen in Figure 1 with a crossflow velocity of 0.4 m s^{-1} ($J_v/k = 1$). After an initial decrease in flux due to osmotic effects, the rate of flux decline is near zero. The rate of flux decline increases with increasing recovery because the solute concentration, and hence the convective transport of mass to the membrane surface, increases.

Effects of solution composition

The role of solution composition appears to be well established, with fouling exacerbated by conditions of low pH (Jucker & Clark, 1994; Hong & Elimelech, 1997; Yuan & Zydney, 1999; Jones &
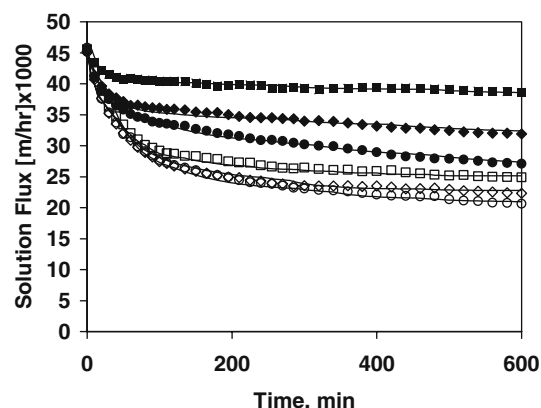

Figure 1. Nanofiltration (NF 70 membrane) of pretreated (microfiltered and softened) Tomhannock reservoir water (14 mg DOC/l) showing the effect of crossflow velocity and recovery ($r = Q_{perm}/Q_{feed}$) on rate of flux decline. Filled symbols, recovery = 75%; open symbols, recovery = 95%. Crossflow velocity: 0.4 m s^{-1} (squares); 0.20 m s^{-1} (diamonds); 0.10 m s^{-1} (circles). Operating conditions: initial solution flux = 1.25×10^{-5} (m s^{-1}), $T = 23$°C.

O'Melia, 2000), high ionic strength (Hong & Elimelech, 1997; Jones & O'Melia, 2000; Yuan & Zydney, 2000), and high divalent cation concentration (i.e., hardness ions) (Hong & Elimelech, 1997; Schafer et al., 1998; Yoon et al., 1998; Yuan & Zydney, 2000).

When rejection of salts is significant, as in NF, flux decline occurs as a result of the osmotic pressure developed, an effect magnified by concentration polarization. In addition, salts can exacerbate membrane compaction and reduce the permeability of charged membranes by reducing the membrane pore size or porosity, due to polymer matrix compaction or shrinkage, caused by an increased ion concentration in the membrane matrix and increased screening of charged moieties (Eriksson, 1988; Braghetta et al., 1997; Kilduff et al., 2004). An alternative explanation postulates an increase in the frictional coefficients inside the membrane (Van Reenen & Sanderson, 1992). Interactions between ionic species and NOM cause greater flux decline than either species acting alone. An example is shown in Figure 2, which shows a statistically significant increase (a factor of about three over the range of ionic strength studied) in the specific resistance of the TMK NOM cake with increasing ionic strength. This corresponds to a significant increase in the rate of NOM
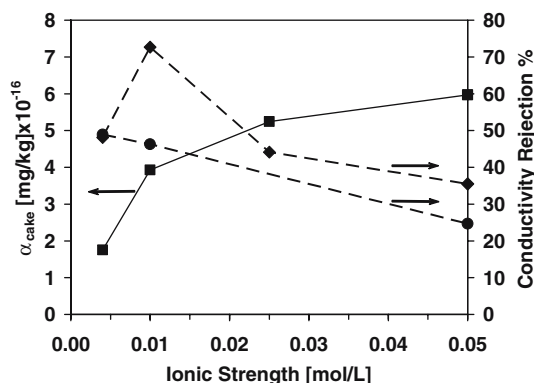
Figure 2. Nanofiltration (NF 70 membrane) of pretreated (microfiltered and softened) Tomhannock reservoir water (10 mg DOC/l). Effect of ionic strength on fitted osmotic pressure/cake formation model specific cake resistance, (squares) and measured conductivity rejection in the presence (diamonds) and absence (circles) of NOM. Operating conditions: initial solution flux $= 1.25 \times 10^{-5}$ (m s^{-1}), crossflow velocity $= 0.1$ (m s^{-1}), recovery $= 0.85$, and $T = 23°C$. Additional details regarding the dataset on which this figure is based can be found in Kilduff et al., 2004a.

solution flux decline. It is likely that the increase in salt concentration in the cake layer reduced charge repulsion between ionized functional groups on single NOM molecules, allowing them to adopt more compact configuration, and between NOM molecules, increasing the compactness of the cake, resulting in lower cake porosity. In separate UF experiments, SEC analysis of UF permeate confirmed a reduction in NOM size with increasing ionic strength (Kilduff et al., 2004b). In addition, the presence of an NOM cake on the membrane surface increased salt rejection (compare diamonds and circles in Figure 2), which increased the effects of osmotic pressure and, in turn, the impact of salt on NOM cake resistance. Rejection decreased with increasing ionic strength as both the membrane charge and the NOM cake charge is shielded more effectively.

Lowering pH and increasing the concentration of divalent cations can also increase the rate of flux decline by reducing NOM charge density and charge repulsion between ionized (acidic) functional groups on NOM molecules, as a result of complex formation, ion pair formation, or both. In addition, cations such as calcium can form bridges between NOM functional groups (Yoon et al., 1998). These effects can result in a more compact cake with higher specific resistance, and

may increase NOM deposition. However, as a result of lower NOM cake charge, and, for negatively charged NF membranes, lower (or shielded) membrane charge (surface and pore), such effects can be mitigated due to a reduction in salt rejection and thus osmotic pressure (Yoon et al., 1998; Kilduff et al., 2004a).

Other factors, including the role of NOM polarity, are less well understood. For example, Carroll et al. (2000) fractionated NOM by charge and polarity and found that the major contribution to fouling was from neutral, hydrophilic NOM components. However, others report that the most extensive membrane fouling was caused by hydrophobic NOM components, as defined by XAD resin adsorption (Nilson & DiGiano, 1996). In addition, as shown in Figure 3, the role of organic matter polarity, as measured by XAD sorption, appears to exhibit a dependency on ionic strength.

Under relatively low ionic strength conditions, flux decline was similar for the unfractionated TMK solution and both the polar and non-polar fractions. In contrast, the hydrophobic fraction, which comprised about 40% of the NOM, exhibited significantly greater flux decline under high
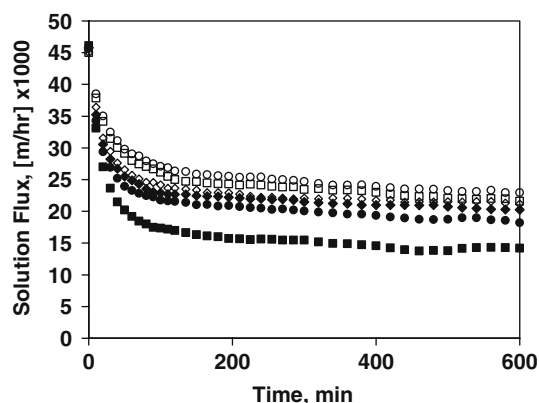

Figure 3. Nanofiltration (NF 70 membrane) of pretreated (microfiltered and softened) Tomhannock reservoir water showing the effect of polarity and ionic strength on flux decline. Filled symbols: 10 mg/l NOM, ionic strength 0.05 M as NaCl. Open symbols; 12 mg/l NOM ionic strength 0.018 M as NaCl. Polarity fraction by XAD sorption: (circles) hydrophilic fraction; (squares) hydrophobic fraction; (diamonds) unfractionated. Operating conditions: initial solution flux $= 1.25 \times 10^{-5}$ (m s^{-1}), crossflow velocity $= 0.1$ (m s^{-1}), recovery $= 0.85$, and $T = 23°C$.

ionic strength conditions. The hydrophobic fraction of the TMK water also had the highest specific UV absorbance, consistent with the findings of others (Schafer et al., 1998). However, recent studies have shown the importance of non-UV absorbing, algogenic polysaccharide material in causing flux decline (Her et al., 2004). These compounds are generally measured as hydrophilic using the XAD sorption protocol. Therefore, the hydrophilic fraction may be comprised of both low molecular weight, charged organic molecules and much higher molecular weight polysaccharides. This could explain why it has been difficult to generalize fouling potential based on polarity, and why different studies find differences in the relative magnitude of flux decline caused by the hydrophilic and hydrophobic fractions.

Role of colloids

Recent research on fouling of microfiltration and ultrafiltration membranes by surface waters has implicated colloids as important foulants. Composition of such colloids may be organic, inorganic, or some combination. For example, Howe and Clark (2002) identified organic matter enriched by Ca and/or Si in lake water foulants using both FTIR and XPS. Yuan and Zydney (1999a, b) showed that convective transport and deposition of relatively large humic acid aggregates catalyzed fouling by smaller humic acid molecules, although their role was less significant for smaller molecular-weight-cutoff (e.g., UF) membranes. Taniguchi et al. (2003c) later showed that surface water NOM could also aggregate and catalyze fouling by smaller NOM molecules, even after pretreatment by microfiltration and softening.

The aggregation of TMK surface water NOM after pretreatment was demonstrated by a bi-modal size distribution measured using membrane fractionation and size exclusion chromatography (SEC) with UV and refractive index detection (Taniguchi et al., 2003c). Greater detail concerning the size and character of these aggregates is shown in Figure 4 (upper panel), which compares SEC chromatograms using UV and multi-angle light scattering (Dawn EOS, Wyatt Technologies, Santa Barbara, CA.) detectors. Low molecular weight components (weight-averaged MW of 1200 based on poly(styrene sulfonate) calibration) were detected by the UV detector. A distinct early-eluting peak composed of non-UV absorbing species was detected by the light scattering detector. The radius of gyration of such species was computed from Debye plots using manufacturer supplied software. As shown in the lower panel of Figure 4, the radius of gyration of NOM aggregates ranges from 50 to over 100 nm, confirming the findings of membrane fractionation experiments and SEC with differential refractometry.

Insight into how aggregates can influence the modes of fouling can be gained by plotting flux data on the coordinates suggested by Equation (1). The slope of versus dt/dW on log-log coordinates yields the filtration constant, n. Such a plot is shown in Figure 5 for filtration by the 1000 kDa membrane (model fits are shown as solid lines, data as symbols). The model predicts that the rate of change of dt/dW plotted on the y-axis increases steeply early in the filtration run, passes through a maximum, and finally reaches a constant value. The filtration constant, n, obtained as the log slope of the model fits shown in Figure 5, progresses from $n = 2$ (indicating pore blockage) early in the filtration run, passes through a transition region, and reaches a plateau value of $n = 0$, indicating that fouling by cake formation controls later in the run. This is consistent with studies that have shown fouling to shift to a cake formation mode after pore blocking processes proceed to completion (Bowen et al., 1995; Lu et al., 1997; Huang & Morrissey, 1998).

The mode of fouling rapidly shifted to cake formation during filtration of the 100 mg/l TMK isolate (shown in Figure 5 as squares). Similar behavior was observed for membranes having MWCOs ranging from 10 to 1000 kDa. In stark contrast, as shown by the single diamond in Figure 5, fouling of the 1000 kDa membrane was essentially eliminated when an additional microfiltration (0.45 micron) step was done just prior to the filtration run, even though the organic carbon concentration was the same. The difference was attributed to the removal of aggregates that formed after pretreatment, as confirmed by both size exclusion chromatography and parallel membrane fractionation. When the TMK solution was diluted by a factor of 2 (shown in Figure 5 as circles), the transition regime between pore blockage and cake formation was reached, but the mode of fouling did not shift fully to cake formation.
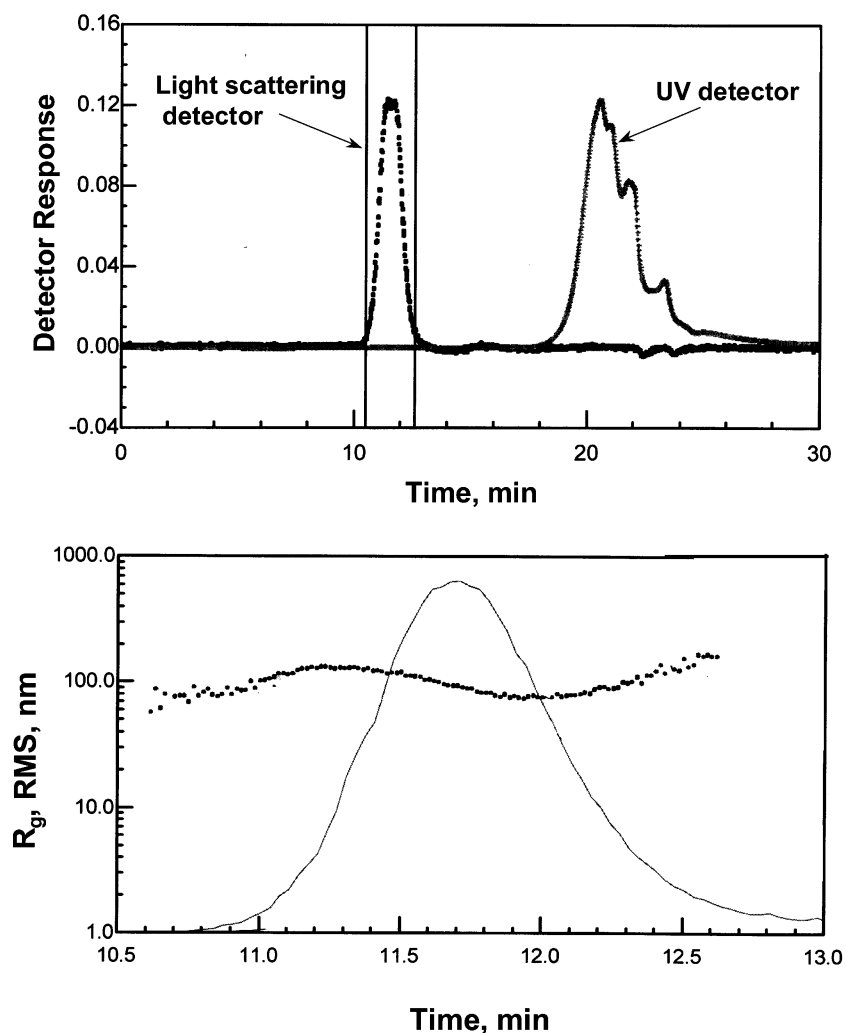
Figure 4. Size exclusion chromatograms of concentrated (100 mg/l) pretreated (microfiltered and softened) Tomhannock reservoir water. Upper panel compares size exclusion chromatograms using UV and multi-angle light scattering detectors. The radius of gyration computed from Debye plots, shown in the lower panel, suggests the existence of non-UV absorbing aggregates.

The shift in fouling mode from cake formation in the presence of NOM aggregates, to pore blockage upon dilution, to lack of fouling after an additional filtration step (and subsequent removal of aggregates) suggests that even though such aggregates comprised a small proportion of the NOM mass, they were responsible for the cake formation on the larger membranes. This supports the findings of Yuan and Zydney (2000), who proposed that an initial fouling layer consisting of large aggregates could effectively 'catalyze' fouling by smaller molecular weight species. In the absence of aggregates, the smaller NOM species penetrated into the membrane pore structure, causing pore blockage instead of forming a cake layer on the surface.

Approaches to mitigate fouling

Several approaches to mitigate the negative effects of NOM fouling on nanofiltration membrane performance have been described (Potts et al., 1981). These include (i) selecting a membrane
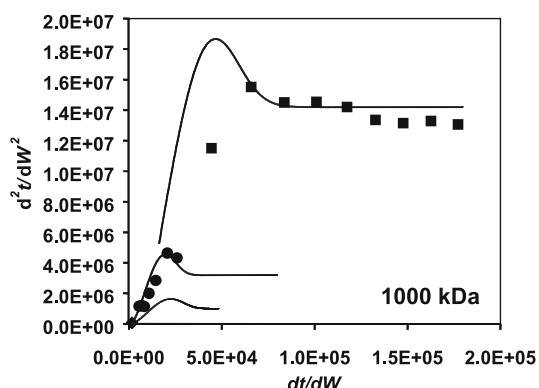
Figure 5. Ultrafiltration (1000 kDa poly(sulfone) membrane) of pretreated (microfiltered and softened) Tomhannock reservoir water. Flux data were plotted on the coordinates of Equation (1). Lines are derivatives calculated from the fitted combined pore blockage-cake formation model (Equations (2) and (3)). The log slope of the plot yields the filtration constant, n. Feed solutions: unfiltered RO isolate (squares) exhibits rapid transition to cake formation ($n = 0$); diluted RO isolate (circles) exhibits pore blockage ($n = 2$); pre-filtered RO isolate (diamonds) showed a lack of fouling. Additional details regarding the dataset on which this figure is based can be found in Taniguchi et al. (2003c).

material that minimizes attractive interactions between NOM and the membrane surface (Childress & Elimelech, 1996); (ii) improved pretreatment to selectively remove the most adhesive components in NOM (Rautenbach et al., 1997); and (iii) enhanced module design and operation that reduces fouling through more effective hydrodynamics, effectively decreasing J_v/k (Chellam & Wiesner, 1997; Mallubhotla & Belfort, 1998). An important variant of (i) above is to tailor membrane surface chemistry for particular applications. Modifications to polymer substrates can be made through homogeneous reaction in solution with subsequent preparation as a synthetic membrane via phase inversion (Nabe et al., 1997). However, an easier, inexpensive, and scalable approach involves surface modification of commercial membranes.

Surface modification

The modification of polymers has found application in several areas. These include such diverse fields as protecting of ship hulls from marine fouling, reducing interactions between the components of blood and implant materials such as catheters, and promoting specific interactions for affinity separation processes and fractionation by chromatography. Heterogeneous graft polymerization of specific functionalities or polymer layers has been employed as a route to tailor polymeric membrane surfaces for many different applications. In contrast to surface modification techniques such as alcohol wetting and surfactant adsorption, graft polymerization can modify membrane surface properties permanently. Applications have included filling membrane pores to improve selectivity of pervaporation membranes (Kai et al., 2000; Yamaguchi et al., 2001); attaching moieties to provide ion-exchange properties (Michel et al., 1998; Saito & Yamashita, 1998; Kim & Saito, 2000); and introducing affinity ligands for protein separations (Kiyohara et al., 1997). Considerable attention has been directed at using graft polymerization to increase the wettability of membrane surfaces as a route to reduce fouling.

Previous research has correlated low surface wettability with non-specific sorption of both detergents and proteins (Sigal et al., 1998). Therefore, graft polymerization to increase the wettability of membrane surfaces offers promise to reduce their ability to interact with species present in solution and thus reduce their potential to foul during filtration. Recent work has shown that it is possible to create nanochannel membranes by grafting amphiphilic copolymers consisting of a poly(vinylidene fluoride) backbone and poly(oxyethylene methacrylate) side chains (Akthakul et al., 2004). These materials were shown to molecularly self-assemble into bicontinuous nanophase domains of semicrystalline PVDF, and poly(ethylene oxide) (PEO), providing selective transport channels of defined size. Fouling resistance was attributed to hydrogen bonding between water and the ether oxygen groups of the PEO side chains, which act as a grafted brush layer at the membrane surface and within the water-filled nanochannels.

Much of the graft polymerization research has been motivated by needs of the biotechnology industry and has focused on reducing the fouling that occurs during ultrafiltration of proteins (e.g., Yamagishi et al. 1995a, b; Ulbricht et al., 1996; Nabe et al., 1997; Chen & Belfort, 1999; Pieracci et al., 1999; Wang et al., 2000; Wavhal & Fisher 2002; Xu et al., 2002). More recently, graft polymerization technology has been applied to

reduce fouling by natural organic materials during potable water production, including reverse osmosis desalination (Belfer et al., 1998; Gilron et al., 2001) and nanofiltration (Kilduff et al., 2000; Freger et al., 2002).

A variety of hydrophilic monomers have been grafted to membrane surfaces to increase their wettability and reduce their potential to foul during filtration. Some of the monomers that have been employed are tabulated in Table 1. Graft polymerization requires the generation of active ionic or radical sites on the membrane surface. This may be accomplished by several different means, including ionizing radiation (Kim et al., 1991; Kiyohara et al., 1997; Kabanov & Kudryavtsev, 2003); oxidants and/or chemical redox systems such as ozone (Wang et al., 2000), benzoyl peroxide (Xu et al., 2002), potassium persulfate-sodium metabisulfite (Belfer et al., 1998), and di-(2-phenoxy ethyl) peroxy dicarbonate (Patil et al., 2001); low temperature helium (Ulbricht & Belfort, 1995, 1996) or argon (Wavhal & Fisher 2002) plasma; and UV radiation (e.g., Yamagishi et al., 1995a, b; Ulbricht et al., 1996, 1998; Pieracci et al., 1999, 2000, 2002).

Modification of poly(aryl sulfones)

In many cases, initiators or specially synthesized molecules having reactive end groups are necessary, often requiring complex reaction conditions and/or long reaction times, both of which increase expense. For example, modification of poly(acrylonitrile) UF membranes via UV radiation required the use of benzophenone as a photoinitiator (Ulbricht et al., 1998); and modification of poly(propylene) MF membranes via ozonation required the use of ferric chloride as an initiator (Wang et al., 2000). It is possible to modify poly(aryl sulfone) membranes without a photoinitiator, as a result of their intrinsic photosensitivity, as described more fully in a US Patent (Crivello et al., 1995). Poly(ether sulfone) membranes offer attractive features for water treatment applications, including wide pH tolerance (1–13) and good resistance to oxidants, including chlorine under water treatment conditions (i.e., < 50 ppm) (Zeman & Zydney, 1996). A possible disadvantage of poly(aryl sulfone) membranes is that they generally exhibit lower wettability (cos $\theta \approx 0.50$–0.60) than both regenerated cellulose (cos $\theta > 0.80$) and commercially available

aromatic polyamide (cos $\theta > 0.80$) membranes. Therefore, poly(aryl sulfone) membranes are potentially more susceptible to fouling by natural organic matter and other colloidal material. Attachment of hydrophilic polymer chains to the membrane surface to significantly increase the wettability of membrane surfaces and reduce fouling is therefore a promising strategy to prepare membranes for water treatment applications.

As shown in Figure 6, when poly(aryl sulfone) membranes are UV-irradiated, the trunk polymer chains are cleaved, forming reactive radical sites. Either water or methanol-soluble monomers chemically bond to these radical sites and undergo free-radical polymerization (Yamagishi et al., 1995a). A potential advantage of UV irradiation is the ability to control trunk polymer bond cleavage (and possible damage to the membrane pore structure) via judicious selection of both the emission intensity and wavelength (Pieracci et al., 2002).

Degree of grafting and grafting efficiency

The wettability of modified membrane surfaces depends on monomer type, monomer concentration and irradiation energy, all factors that govern the amount of polymer grafted to the surface. The amount of polymer grafted, or the 'degree of grafting' may be assessed gravimetrically (e.g., Yamagishi et al., 1995a) and by spectroscopic techniques. For example, the degree of grafting, DG, was determined by Taniguchi et al. (2003a, b) using attenuated total reflectance Fourier Transform infrared spectroscopy (ATR/FTIR). DG was defined as the ratio of the peak height due to absorbance of the carbonyl group of the grafted molecule to that at 1487 cm^{-1} due to the absorbance by the benzene carbon–carbon bond (which remained unaffected by grafting) minus the value of that ratio for the unmodified membrane (possibly caused by additives in the original casting mixture). Degree of grafting generally increases with monomer solution concentration, which is usually on the order of 1–5% w/w (Ulbricht et al., 1996; Pieracci et al., 2000). It will also increase with applied energy dosage (J m^{-2}) (controlled by light intensity and radiation time), but may exhibit a plateau or a maximum as depletion of available monomer and/or loss (cleavage or ablation) of grafted monomer occurs at high energy dosages (Taniguchi et al., 2003b). Taniguchi et al. (2003b) found a linear

Table 1. Hydrophilic monomers that have been grafted to membrane surfaces to increase surface wettability and reduce fouling potential during filtration
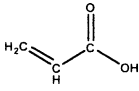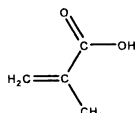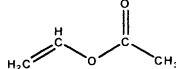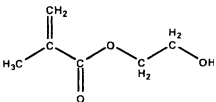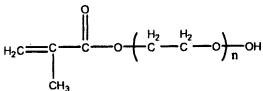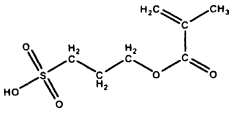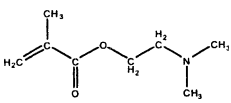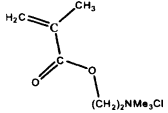
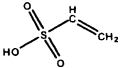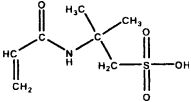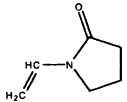| Monomer	Abbr.	Structure	References
Acrylic acid	AA		Ulbricht and Belfort (1996), Ulbricht et al. (1996, 1998), Freger et al. (2002), Wavhal and Fisher (2002), Xu et al. (2002), Taniguchi et al. (2004)
Methacrylic acid	MA		Yamagishi et al. (1995b), Ulbricht and Belfort (1996), Belfer et al. (1998, 1999, 2000), Freger et al. (2002)
Vinyl acetate	VA		Kim et al. (1991)
2-Hydroxyethyl methacrylate	HEMA		Yamagishi et al. (1995b), Ulbricht and Belfort (1996), Ulbricht et al. (1996), Wang et al. (2000), Taniguchi et al. (2004)
Poly(ethylene glycol) methacrylate	PEG-MA		Ulbricht et al. (1996, 1998), Belfer et al. (1998b, 2000, 2001); Gilron et al. (2001), Freger et al. (2002)
3-sulfopropyl methacrylate	SPMA		Belfer et al. (1998b, 1999, 2000, 2001), Gilron et al. (2001), Freger et al. (2002), Taniguchi et al. (2004)
2-dimethylamino-ethyl methacrylate	AEMA		Ulbricht et al. (1998)
2-trimethyl ammonium-ethyl methacrylate chloride	AmEMA		Ulbricht et al. (1998)
Vinylsulfonic acid	VSA		Belfer et al. (1998b)

Table 1. Continued

Monomer	Abbr.	Structure	References
2-acrylamido-2-methyl-1-propane sulfonic acid	AMPS		Belfer et al. (1998b), Gilron et al. (2001), Taniguchi et al. (2004)
N-Vinyl-2-pyrrolidone	NVP		Chen and Belfort (1998); Pieracci et al. (1999, 2000, 2002), Kilduff et al. (2000)

correlation between DG and the product of monomer concentration and irradiation energy, $C \times E$ (wt% kJ m^{-2}), for the NVP/PES system for $C < 10\%$ w/w and $E < 4$ kJ m^{-2}.

Grafting efficiency, the DG achieved at a given energy dosage, also depends on UV wavelength. The efficiency of grafting *N*-vinyl pyrolidinone onto PES membranes was significantly higher with high-energy 254 nm lamps as compared to 300 nm lamps (Pierraci et al., 2002a). However, the high-energy wavelength was also responsible for rapid pore enlargement and loss of rejection for bovine serum albumin. Rejection was better maintained when the higher wavelength lamps were used, and could be further optimized by using filters (e.g., benzene) to tailor the wavelengths reaching the membrane surface.

The degree of grafting achieved for a given lamp wavelength and energy dosage will depend on both the sensitivity of the base polymer, and intrinsic
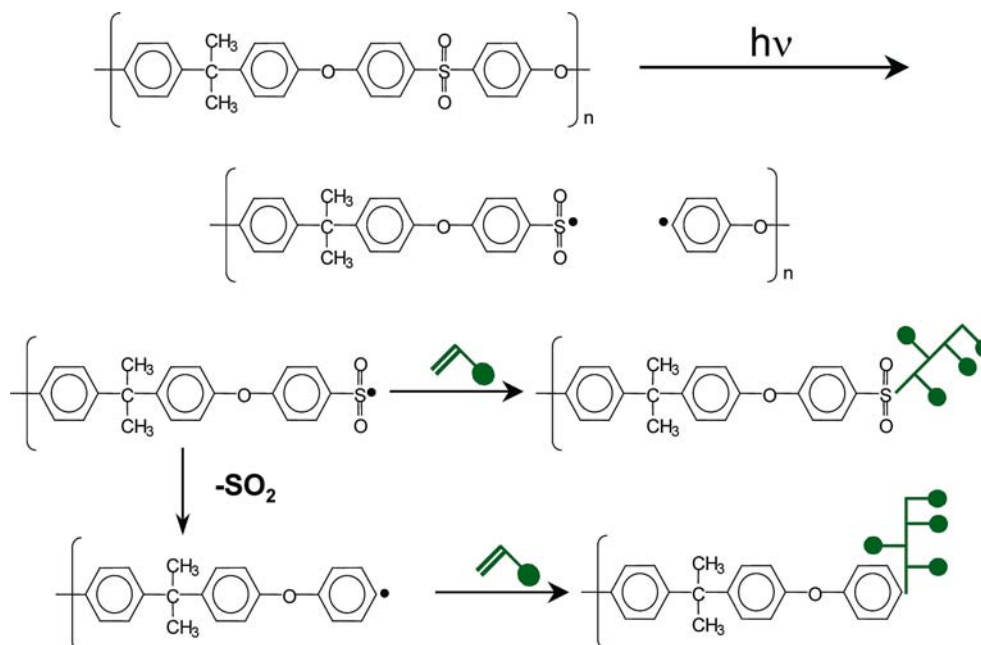

Figure 6. Proposed mechanism of UV-assisted graft polymerization of poly(aryl sulfone) membranes showing trunk polymer cleavage, formation of reactive radical sites, and chain growth (after Yamagishi et al., 1995a).

properties of the monomers employed. Kaeselev et al. (2001) observed significant differences in the initial polymerization rate and the degree of grafting for several hydrophilic monomers, including NVP and AMPS (see Table 1). Furthermore, much higher irradiation energy was required to achieve a desired degree of grafting when polysulfone was the base polymer as compared with poly(ether sulfone).

Ideally, monomer will bond exclusively to either the surface or polymer chains, and homopolymer formation will be minimized, because homopolymerization consumes monomer and the polymer particles formed could become trapped in pores, reducing membrane permeability. Such homopolymer will contribute to the measured degree of grafting whether gravimetric or spectroscopic techniques are used. Ethanol washing has been used to remove homopolymer from membrane pores, and to assess the degree of homopolymerization (Pierracci et al., 2002b; Taniguchi et al., 2003b). The degree of grafting is lower when modified membranes are post-washed in ethanol, but the difference is only significant above a critical irradiation energy. For the NVP/PES system, this energy is in the range of 4–5 kJ m^{-2}; energy doses below this value do not promote homopolymerization and the post-wash technique does not have any effect on the degree of grafting. This is somewhat lower than the observed maxima in DG as a function of applied energy dosage.

Degree of grafting and wettability

The ability of graft polymerization to achieve a significant reduction in contact angle, θ, and increase in wettability (cos θ) relative to as-received (unmodified) membranes is shown in Figure 7. Membranes made from sulfonated polysulfone and poly(ether sulfone) were modified with a 3% solution of N-vinyl pyrolidinone. Contact angle was reduced by up to 50% relative to as-received membranes, and could be reduced to values approaching regenerated cellulose (the 'gold standard' of wettability) and well below that of a widely used aromatic polyamide thin film composite membrane. Similar results have been obtained using the NVP/PES system (Pieracci et al., 1999, 2000, 2002a); using other hydrophilic monomers with PES (Yamagishi et al., 1995b; Kaeselev et al., 2001; Taniguchi et al., 2003a, b, 2004); and using
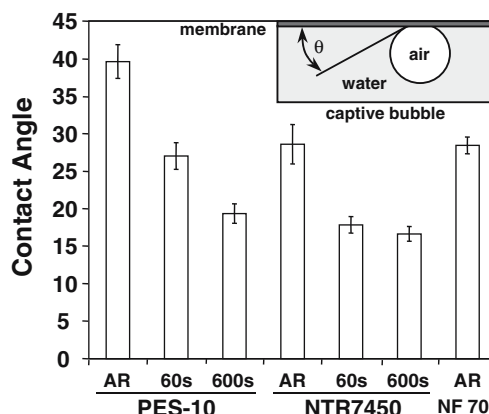

Figure 7. Effect of graft polymerization on membrane wettability. Graft modification of PES-10 poly(ether sulfone) and NTR 7450 sulfonated polysulfone membranes with 3% w/w N-vinyl pyrolidinone for various times, as indicated. Significant reduction in contact angle was achieved relative to as-received membranes (AR) and a commercial aromatic polyamide thin film composite membrane (NF 70). Additional details regarding the dataset on which this figure is based can be found in Kilduff et al. (2002).

other monomer/base polymer materials. For example, Ulbricht et al. 1996 modified PAN with acrylic acid and PEG methacrylates, whereas Kim et al. (2002) modified PVC with NVP; both studies observed significant increase in wettability.

The wettability of modified membranes generally increases with increasing DG, but often exhibits asymptotic behavior (Kaeselev et al., 2001; Kilduff et al., 2002; Pierraci et al., 2002a; Taniguchi et al., 2004). The asymptote value, and the rate of approach toward this value, both depend on the intrinsic properties of the monomers employed (Kaeselev et al., 2001; Taniguchi et al., 2004), but values on the order of 0.85–0.90 are readily attainable and are comparable to regenerated cellulose (cosθ = 0.91 (Pieracci et al., 2002a). Taniguchi et al. (2004) observed that larger monomers reached their maximum wettability values at lower values of DG than smaller molecules, possibly because each molecule covers a greater proportion of the membrane surface. However, smaller monomers were more reactive, either because of their increased diffusivity or intrinsic properties. Reactivity, defined as the initial slope of a plot of DG versus the product of monomer concentration and irradiation time, Ct, decreased with the cube root of monomer

molar volume. Experience thus far suggests that relatively low DG values (0.2 to less than 1) and intermediate wettabilities ($0.74 < \cos\theta < 0.82$) are sufficient to produce membrane surfaces that resist fouling by both proteins and natural organic matter (Kaeselev et al., 2001; Kilduff et al., 2002; Taniguchi et al., 2003a, b).

In one approach to modifying membranes (dip technique), coupons are dipped in monomer solution (e.g., for about 30 min), and then irradiated in nitrogen. An alternative is the immersion method, in which membrane coupons are irradiated while immersed in monomer solution. For a given degree of grafting, these two methods produced similar surface wettability (Kilduff et al., 2002), and both methods could produce membranes with the same wettability as regenerated cellulose (Pierraci et al., 2000). However, the kinetics of the dip technique were superior. For example, a high degree of grafting of N-vinyl-2-pyrrolidone to a 50 kDa poly(ether sulfone) membrane was realized in 30 s using the dip method, whereas 300 s were required to achieve a similar degree of grafting using the immersion technique (Pierraci et al., 2000). In large part, this is because the N-vinyl-2-pyrrolidone solution absorbed much of the UV energy, shielding the membrane, and thus required long irradiation times.

Effect of grafting on surface roughness and permeability

Surface roughness may influence fouling, when the relative scale of the roughness and the size of solution components are similar. Ulbricht et al. (1998) found that thin polymer layers of certain acrylates and methacrylates grafted onto PAN reduced surface roughness and decreased advancing/receding contact angle hysteresis. However, not all grafted monomers resulted in a smoother surface, and inhomogeneities were observed. These may have been created by gel-formation, agglomeration and precipitation during modification. Pieracci et al. (1999) found that UV irradiation of 10 kDa poly(ethersulfone) UF membranes (using a wavelength of 254 nm) increased their roughness (measured using AFM) by 0.6–1.1 nm, on the order of 50 to nearly 100%. Subsequent graft polymerization of N-vinyl-2-pyrrolidone appeared to smooth out this roughness, depending on the degree of

monomer grafting. Taniguchi et al. (2003b) investigated the effect of graft polymerization on surface roughness as a function of applied energy dosage. Using lower energy 300 nm lamps, Taniguchi et al. (2003b) observed lower increase in roughness in the absence of graft polymerization than the Pieracci et al. (1999) study. Consistent with that work, roughness decreased with increasing energy dosage, until a minimum was reached, and then increased. The minimum in surface roughness was generally smoother than the as-received membranes, and corresponded to the maxima in DG. As chain scission, homopolymerization, and surface etching became more important than photo-induced grafting at high-energy values, roughness increased. The effect of irradiation on roughness appeared to correlate with membrane skin thickness; roughness increased to a significantly greater extent for membranes having a thin skin (2 μm) as compared to those having a thicker skin (8 μm).

Kilduff et al. (2002) fitted the pore blockage/cake formation model to flux data for filtration of NOM solutions by NVP graft-modified PES membranes for different reaction times. The fitted pore blockage parameter (Equation (2)) for the membrane irradiated for the longest period of time (180 s, using 254 nm lamps) was significantly higher than the fitted value for all other membranes, providing evidence that increased surface roughness may exacerbate fouling and/or change the fouling mechanism. However, the effect of roughness on fouling may be largely physical, related to the ability of foulants to become lodged in pores, and not related to adsorption effects. Han et al. (2004) showed that root mean square roughness ranging from 5 to 60 nm had little effect on hen egg lysozyme adsorption, and speculated that surface roughness would only affect the sorption of protein when the average length scale of the substrate surface is of the same size or smaller than the dimension of the adsorbate (although changes in orientation may be possible). When the scale of the roughness exceeds that of the protein dimension, the chemical composition of the substrate surface has a *dominant* influence on the adsorption process.

Graft polymerization has been shown to reduce membrane permeability (increase membrane resistance) (Ulbricht et al., 1996; Pieracci et al., 2000; Kaeselev et al., 2002; Kilduff et al., 2002; Taniguchi et al., 2003a, b, 2004). A reduction of up to about 40–60% after graft modification of commercial

PES-10 poly(ether sulfone) with 3% w/w *N*-vinyl pyrolidinone as compared to as-received NF-PES-10 membranes is shown in Figure 8 for irradiation times of 60 s and 10 s, respectively. A reduction in permeability is explained by pores blocked by grafted poly(vinyl pyrolidinone) (PVP) chains, and possibly some homopolymer deposition in pores. Figure 8 also shows data illustrating an increase in permeability at longer irradiation times. In this study, a decline in the degree of grafting with increasing irradiation time was not observed; therefore, exhaustion of monomer on the membrane surface and subsequent trunk polymer scission is not a likely explanation. A more likely explanation is the loss (cleavage or ablation) of grafted monomer at long irradiation times.

Effect of grafting on rejection and cleaning

Graft polymerization can induce significant increases in rejection for natural organic matter (Kilduff et al., 2002; Taniguchi et al., 2003a). A decrease in permeability and concomitant increase in rejection suggest that grafted polymers are constricting pores, blocking pores, or both, shifting the pore size distribution to smaller sizes. In addition, when grafted monomers contain acidic groups,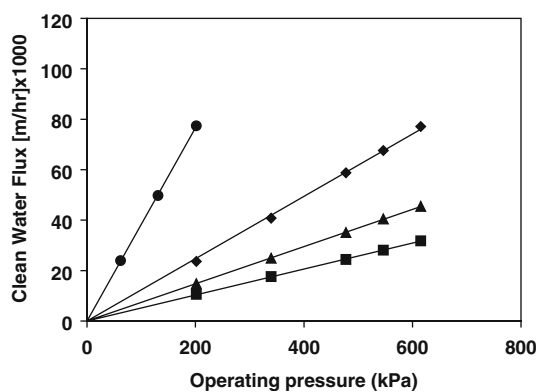 an increase in rejection may be caused, in part, by electrostatic repulsion between charge moieties on NOM molecules and acidic groups on the grafted polymers. Taniguchi et al. (2003a) found that rejection of NOM by membranes grafted with two neutral polymers, HEMA and NVP was lower than membranes grafted with monomers containing carboxylic or sulfonic acid groups (see Table 1). It is also possible for rejection to decrease as a result of graft modification.

Two factors may contribute to a decrease in rejection. When high-energy wavelengths are used, trunk polymer scission, rapid pore widening and cleavage of grafted monomers can dominate over photo-induced grafting when irradiation times are too long. Second, some monomer solutions may have the ability to swell and even dissolve the base polymer material, which can reduce rejection (Taniguchi et al., 2004). When PES is the base polymer material, both NVP and HEMA (although to a lesser extent) have shown this ability. Kaeselev et al. (2002) observed a simultaneous decrease in volume flux and retention of dextran by PES membranes modified with AAG and AAP using high-energy 254 nm lamps. They explained the increase in hydrodynamic resistance as resulting from an increase in cross-linking, while chain scission was seen as responsible for loss of selectivity.

Kilduff et al. (2002) showed that it was possible to both increase solute rejection and decrease the rate of flux decline during filtration of NOM solutions via graft polymerization with NVP. However, total fouling by NOM, caused by the accumulation of rejected solute on the surface of the membranes (cake formation), is strongly related to solute rejection, consistent with previous reports. An increase in the cake formation parameter, determined by fitting Equations (2) and (3) to NOM flux data using PES membranes modified with 3% NVP, is shown in Figure 9 to correlate with increasing rejection. The increase in rejection was due to graft modification of commercial PES-10 poly(ether sulfone) membranes with 3% w/w *N*-vinyl pyrolidinone using the dip method with 254 nm lamps for irradiation time ranging from 10 to 180 s. The behavior of total NOM fouling as a function of rejection, which varied over a wide range (0–0.80), was interpreted by Taniguchi et al. (2003a) in the context of the NOM molecular weight distribution of the NOM. Large changes in total fouling occurred when changes in the membrane pore size due to grafting

Figure 8. Effect of graft polymerization on membrane permeability. Graft modification of commercial PES-10 poly(ether sulfone) with 3% w/w *N*-vinyl pyrolidinone using the dip method with 254 nm lamps for various times: (diamonds) 0 s, $L_p = 0.124$ m/(hr-kPa); (squares) 10 s, $L_p = 0.052$ m/(hr-kPa); (triangles) 60 s, $L_p = 0.074$ m/(hr-kPa); (circles) 180 s, $L_p = 0.383$ m/(hr-kPa). Additional details regarding the dataset on which this figure is based can be found in Kilduff et al. (2002).
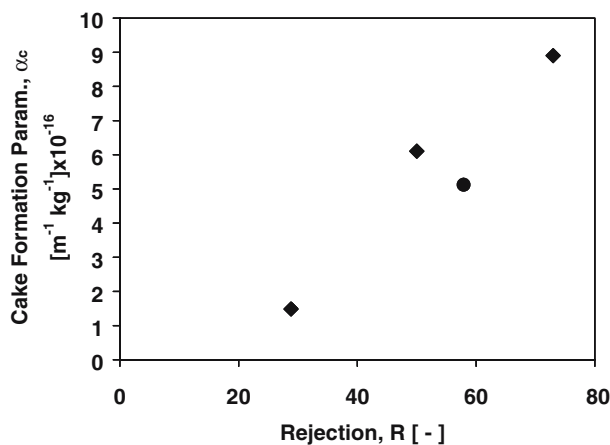
Figure 9. Effect of rejection on the cake formation parameter determined by fitting Equations (2) and (3) to flux data. (circle) as-received, unmodified commercial PES-10 poly(ether sulfone) membrane; (diamonds) graft modification of membranes with 3% w/w *N*-vinyl pyrolidinone using the dip method with 254 nm lamps for 10–180 s. Additional details regarding the dataset on which this figure is based can be found in Kilduff et al. (2002).

corresponded to regions of the solute molecular size distribution that contained a large proportion of the solute mass.

An important goal of graft modification is to produce membranes that exhibit reduced irreversible fouling by NOM and that are easier to clean using a minimum of chemical agents. As-received PES membranes required a combination of hydrodynamic cleaning with water followed by chemical cleaning with NaOH to recover the same fraction (98%) of the initial flux as that achieved by cleaning the NVP-modified membrane with water only (Kilduff et al., 2002). Taniguchi et al. (2003a) found that irreversible fouling was significantly affected by the membrane surface chemistry, and that PES membranes grafted with acrylic acid were able to reduce irreversible fouling to zero (shown in Figure 10). However, as shown in Figure 10, the wettability (or hydrophilicity) of modified surfaces alone was not a good predictor of reduced fouling potential; monomers such as HEMA and AAG resulted in a significant increase in irreversible fouling even though they are strongly hydrophilic. One possible explanation is that because NOM is structurally and chemically heterogeneous, adsorption of specific functional groups may be enhanced even though the surface itself is more wettable. More work is needed to identify monomers appropriate for reducing NOM fouling, and to develop criteria to predict their effectiveness.

Conclusions

Flux decline caused by natural water foulants may result from concentration polarization, from pore blockage by solute adsorbed on the membrane surface or within pores, and from the formation of a cake layer on the membrane surface, which presents a resistance to flow in addition to the membrane itself. Rate models that combine pore blockage and cake filtration have successfully described flux decline when salt concentration polarization is negligible, although more work is needed to relate foulant properties to model parameters – specific cake resistance and the pore blockage rate constant. In addition, when rejection of salts is significant, as in NF and RO, flux decline occurs as a result of the osmotic pressure developed. Salts can also exacerbate membrane compaction, reduce the permeability of charged membranes, and reduce charge repulsion between ionized functional groups on single NOM molecules, increasing the compactness of NOM cakes. Lowering pH and increasing the concentration of divalent cations can also increase the rate of flux decline by reducing NOM charge density, as a result of complex formation, ion pair formation, or both. In addition, cations such as calcium can form bridges between NOM functional groups. These effects can result in a more compact cake with higher specific resistance, and may increase NOM deposition. However, such effects can be partially mitigated due to a reduction in salt
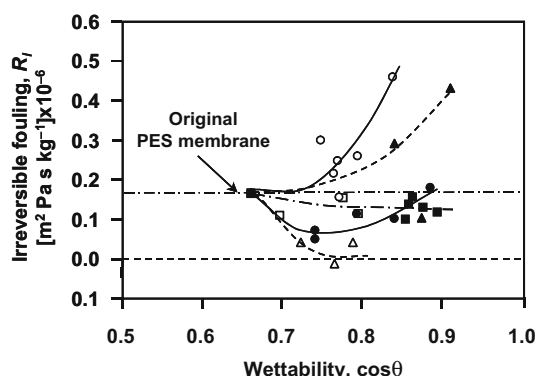
Figure 10. Irreversible resistance R_I ($= R_F - R_M$) versus wettability after NOM filtration by PES membranes modified with hydrophilic monomers: (open circles) HEMA; (filled circles) NVP; (open triangles) AA; (filled triangles) AAG; (open squares) SPMA; (filled squares) AMPS. Additional details regarding the dataset on which this figure is based can be found in Taniguchi et al. (2003a).

rejection, and thus osmotic pressure. The role of polarity is difficult to generalize. Large, aromatic components measured as hydrophobic by adsorption to methyl methacrylate resin at low pH have been shown to contribute to fouling, but non-UV absorbing, algogenic polysaccharide material measured as hydrophilic using the same protocol also cause significant flux decline. The presence of colloids and/or aggregates, which may contain both organic and inorganic components, can play an important role in fouling. They can govern the type of fouling observed, and can catalyze fouling by smaller molecules. In addition, aggregates may form during filtration even after pretreatment as concentrations of dissolved and colloidal matter increase.

Minimizing interactions between foulants and membrane surfaces is an important strategy for mitigating fouling during filtration. Graft polymerization is a versatile technique to minimize such interactions by producing membranes having a wide range of surface properties, including charge density and wettability, via selection of monomer properties and functionality. Through judicious choice of starting pore size, monomer type, and graft polymerization conditions (UV intensity, wavelength energy, irradiation time, and monomer concentration), flux and rejection can be tailored for different applications. Charged membranes, which incorporate Donnan exclusion in addition to size exclusion, can significantly enhance the rejec-

tion of NOM. Major benefits of surface modification include a reduction in fouling due to adsorption of NOM, which is likely to be most important for high-humic content waters, and a reduction or elimination of irreversible fouling, making cleaning protocols more effective and possibly chemical-free. A major fouling mechanism for NOM is cake formation; more work is needed to identify ways in which modified surfaces can influence cake properties. More research is also needed to identify additional monomers appropriate for reducing NOM fouling, to develop criteria to predict their effectiveness, and to evaluate their effectiveness for preventing fouling by polysaccharide-rich algogenic organic matter.

Acknowledgements

References

Aiken G.R. & R.L. Malcolm, 1987. Molecular weight of aquatic fulvic acids by vapor pressure osmometry, Geochim. Cosmochim. Acta 51, 2177.

Aiken G.R., D.M. McKnight, K.A. Thorn & E.M. Thurman, 1992. Isolation of hydrophilic organic acids from water using nonionic macroporous resins, Org. Geochem. 18, 567–573.

Alborzfar M., G. Jonsson & C. Gron, 1998. Removal of natural organic matter from two types of humic groundwaters by nanofiltration, Water Res. 32, 2983–2994.

Allegeir S.C. & R.S. Summers, 1995. Evaluating NF for DBP control with the RBSMT, J. AWWA 87, 87–99.

Akthakul A., R.F. Salinaro & A.M. Mayes, 2004. Antifouling polymer membranes with subnanometer size selectivity, Macromolecules 37, 7663–7668.

Beckett R., Z. Jue & C. Giddings, 1987. Determination of molecular weight distributions of fulvic and humic acids

542

using flow field-flow fractionation, Environ. Sci. Technol. 21, 289–295.

Belfer S., Y. Purinson, R. Fainshtein, Y. Radchenko & O. Kedem, 1998. Surface modification for commercial composite polyamide reverse osmosis membranes, J. Membrane Sci. 139, 175–181.

Blau T.J., J.S. Taylor, K.E. Morris & L.A. Mulford, 1992. DBP control by nanofiltration: cost and performance, J. AWWA 84, 104–116.

Bowen W.R., J.I. Calvo & A.J. Hernandez, 1995. Steps of membrane blocking in flux decline during protein microfiltration, J. Membrane Sci. 101, 153–165.

Braghetta A., F.A. DiGiano & W.P. Ball, 1997. Nanofiltration of natural organic matter: pH and ionic strength effects, J. Environ. Eng. 123, 628–641.

Braghetta A., F.A. DiGiano & W.P. Ball, 1998. NOM accumulation at NF membrane surface: impact of chemistry and shear, J. Environ. Eng. 123, 1087–1098.

Buffle J., 1990. The analytical challenge posed by fulvic and humic acids, Anal. Chim. Acta 232, 1–2.

Cameron R.S., B.K. Thornton, R.S. Swift & A.M. Posner, 1972. Molecular weight and shape of humic acid from sedimentation and diffusion measurements on fractionated extracts, J. Soil Sci. 23, 394–408.

Carroll T., S. King, S.R. Gray, B.A. Bolto & N.A. Booker, 2000. Fouling of microfiltration membranes by NOM after coagulation treatment, Water Res. 34, 2861–2868.

Chellam S., 2000. Effects of nanofiltration on trihalomethane and haloacetic acid precursor removal and speciation in waters containing low concentrations of bromide ion, Environ. Sci. Technol. 34, 1813–1820.

Chellam S. & M.R. Wiesner, 1997. Particle back-transport and permeate flux behavior in crossflow membrane filters, Environ. Sci. Technol. 31, 819–824.

Chen H. & G. Belfort, 1999. Surface modification of poly(ether sulfone) ultrafiltration membranes by low-temperature plasma-induced graft polymerization, J. Appl. Polym. Sci. 72, 1699–1711.

Childress A.E. & M. Elimelech, 1996. Effect of solution chemistry on the surface charge of polymeric reverse osmosis and nanofiltration membranes, J. Membrane Sci. 119, 253–268.

Chin Y.P. & P.M. Gschwend, 1991. The abundance, distribution, and configuration of porewater organic colloids in recent sediments, Geochim. Cosmochim. Acta 55, 1309–1317.

Chin Y.P., G. Aiken & E. O'Laughlin, 1994. Molecular weight, polydispersity, and spectroscopic properties of aquatic humic substances, Environ. Sci. Technol. 28, 1853–1858.

Cho G.A. & J. Pellegrino, 1999. Membrane filtration of natural organic matter: initial comparison of rejection and flux decline characteristics with ultrafiltration and nanofiltration membranes, Water Res. 33, 2517–2526.

Cho G., G. Amy & J. Pellegrino, 2000a. Membrane filtration of natural organic matter: comparison of flux decline, NOM rejection, and foulants during filtration with three UF membranes, Desalination 127, 283–298.

Cho J., G. Amy & J. Pellegrino, 2000b. Membrane filtration of natural organic matter: factors and mechanisms affecting

rejection and flux decline with charged ultrafiltration (UF) membrane, J. Membrane Sci. 164, 89–110.

Combe C., E. Molis, P. Lucas, R. Riley & M.M. Clark, 1999. The effect of CA membrane properties on adsorptive fouling by humic acid, J. Membrane Sci. 154, 73–87.

Cornel P.K., R.S. Summers & P.V. Roberts, 1986. Diffusion of humic acid in aqueous solution, J. Colloid Interf. Sci. 110, 149–164.

Crivello J.V., G. Belfort & H. Yamagishi, 1995. Low fouling ultrafiltration and microfiltration aryl polysulfone. US Patent Number 5,468,390, United States.

Eriksson P., 1988. Nanofiltration extends the range of membrane filtration, Environ. Prog. 7, 58–62.

Freger V., J. Gilron & S. Belfer, 2002. TFC polyamide membranes modified by grafting of hydrophilic polymers: an FT-IR/AFM/TEM study, J. Membrane Sci. 209, 283–292.

Gilron J., S. Belfer, M. Vaisanen & M. Nystrom, 2001. Effects of surface modification on antifouling and performance properties of reverse osmosis membranes, Desalination 140, 167–179.

Han M., A. Sethuraman, R.S. Kane & G. Belfort, 2004. Nanometer-scale roughness having little effect on the amount or structure of adsorbed protein, Langmuir 19, 9868–9872.

Her N., G. Amy, H.-R. Park & M. Song, 2004. Characterizing algogenic organic matter (AOM) and evaluating associated NF membrane fouling, Water Res. 38, 1427–1438.

Hermia J., 1982. Constant pressure blocking filtration laws – application to power law non-Newtonian fluids, Trans. Inst. Chem. Eng. 60, 183–187.

Ho C.C. & A.L. Zydney, 2000. A combined pore blockage and cake filtration model for protein fouling during microfiltration, J. Colloid Interf. Sci. 232, 389–399.

Hong S. & M. Elimelech, 1997. Chemical and physical aspects of natural organic matter (NOM) fouling of nanofiltration membranes, J. Membrane Sci. 132, 159–181.

Howe K.J. & M.M. Clark, 2002a. Fouling of microfiltration and ultrafiltration membranes by natural waters, Environ. Sci. Technol. 36, 3571–3576.

Howe K.J., K.P. Ishida & M.M. Clark, 2002b. Use of ATR/FTIR spectrometry to study fouling microfiltration membranes by natural waters, Desalination 147, 251–255.

Huang L. & M.T. Morrissey, 1998. Fouling of membranes during microfiltration of surimi wash water: roles of pore blocking and surface cake formation, J. Membrane Sci. 144, 113–123.

Jones K.L. & C.R. O'Melia, 2000. Protein and humic acid adsorption onto hydrophilic membrane surfaces: effects of pH and ionic strength, J. Membrane Sci. 165, 31–46.

Jucker C. & M.M. Clark, 1994. Adsorption of aquatic humic substances on hydrophobic ultrafiltration membranes, J. Membrane Sci. 97, 37–52.

Kabanov V.A. & V.N. Kudrayavtsev, 2003. Modification of polymers by radiation graft polymerization (State of the Art and Trends), High Energy Chem. 37, 1–5.

Kabsch-Korbutowicz M., K. Majewska-Nowak & T. Winnicki, 1999. Analysis of membrane fouling in the treatment of water solutions containing humic acids and mineral salts, Desalination 126, 179–185.

Kaeselev B., J. Pieracci & G. Belfort, 2001. Photoinduced grafting of ultrafiltration membranes: comparison of

poly(ether sulfone) and poly(sulfone), J. Membrane Sci. 194, 245–261.

Kaeselev B., P. Kingshott & G. Jonsson, 2002. Influence of the surface structure on the filtration performance of UV-modified PES membranes, Desalination 146, 265–271.

Kai T., T. Tsurum, S.-I. Nakao & S. Kimura, 2000. Preparation of hollow-fiber membranes by plasma-graft filling polymerization for organic-liquid separation, J. Membrane Sci. 170, 61–70.

Kaiya Y., Y. Itoh, K. Fujita & S. Takizawa, 1996. Study on fouling materials in the membrane treatment process for potable water, Desalination 106, 71–77.

Kilduff J.E., S. Mattaraj, J.P. Pieracci & G. Belfort, 2000. Photochemical modification of poly(ether sulfone) and sulfonated poly(sulfone) nanofiltration membranes for control of fouling by natural organic matter, Desalination 132, 133–142.

Kilduff J.E., S. Mattaraj, J. Sensibaugh, J.P. Pieracci, Y.X. Yuan & G. Belfort, 2002. Modeling flux decline during nanofiltration of NOM with poly(arylsulfone) membranes modified using UV-assisted graft polymerization, Environ. Eng. Sci. 19, 477–495.

Kilduff J.E., S. Mattaraj & G. Belfort, 2004a. Flux decline during nanofiltration of naturally-occurring dissolved organic matter: effects of osmotic pressure, membrane permeability, and cake formation, J. Membrane Sci. 239, 39–53.

Kilduff J.E., S. Mattaraj, A. Wigton, M. Kitis & T. Karanfil, 2004b. Effects of reverse osmosis isolation on reactivity of naturally occurring dissolved organic matter in physicochemical processes, Water Res. 38, 1026–1036.

Kim M., K. Saito & S. Furusaki, 1991. Water flux and protein adsorption of a hollow fiber modified with hydroxyl groups, J. Membrane Sci. 56, 289–302.

Kim M. & K. Saito, 2000. Radiation-induced graft polymerization and sulfonation of glycidyl methacrylate on to porous hollow-fiber membranes with different pore sizes, Radiat. Phys. Chem. 57, 167–172.

Kim D.S., J.S. Kang, K.Y. Kim & Y.M. Lee, 2002. Surface modification of a poly(vinyl chloride) membrane by UV irradiation for reduction in sludge adsorption, Desalination 146, 301–305.

Kiyohara S., M. Kim, Y. Toida, K. Saito, K. Sugita & T. Sugo, 1997. Selection of a precursor monomer for the introduction of affinity ligands onto a porous membrane by radiation-induced graft polymerization, J. Chromatogr. A 758, 209–215.

Krasner S.W., J.J. Westrick & S. Regli, 1995. Bench and pilot testing under the ICR, J. AWWA 8, 60–68.

Leenheer J.A., 1981. Comprehensive approach to preparative isolation and fractionation of dissolved organic-carbon from natural-waters and wastewaters, Environ. Sci. Technol. 15, 578–587.

Leenheer J.A., J.-P. Croue, M. Benjamin, G.V. Korshin C.J. Hwang, A. Bruchet & G.R. Aiken, 2000. Comprehensive isolation of natural organic matter from water for spectral characterizations and reactivity testing. ACS Symposium Series, 761.

Leenheer J.A. & J.P. Croue, 2003. Characterizing aquatic dissolved organic matter, Environ. Sci. Technol. 37, 18A–26A.

Lin C.-F., Y.-J. Huang & O.J. Hao, 1999. Ultrafiltration processes for removing humic substances: effect of molecular weight fractions and PAC treatment, Water Res. 33, 1252–1264.

Lin C.-F., T.-Y. Lin & O.J. Hao, 2000. Effects of humic substance characteristics on UF performance, Water Res. 34, 1097–1106.

Lu W.M., K.L. Tung & K.J. Hwang, 1997. Effect of woven structure on transient characteristics of cake filtration, Chem. Eng. Sci. 52, 1743–1756.

Maartens A., P. Swart & E.P. Jacobs, 2000. Membrane pretreatment: a method for reducing fouling by natural organic matter, J. Colloid Interf. Sci. 221, 137–142.

Malcolm R.L., 1990. The uniqueness of humic substances in each of soil stream and marine environments, Anal. Chim. Acta 232, 19–30.

Malcolm R.L. & P. MacCarthy, 1992. Quantitative evaluation of XAD-8 and XAD-4 resins used in tandem for removing organic solutes from water, Environ. Int. 18, 597–607.

Mallevialle J., C. Anselme & O. Marsigny,. 1989. Effects of Humic Substances on Membranes Processes Aquatic Humic Substances, Influence on Fate and Treatment of Pollutants. Washington, D.C: I. H. S. a. P. McCarthy.

Mallubhotla H. & G. Belfort, 1998. Semiempirical modeling of cross-flow microfiltration with periodic reverse filtration, Ind. Eng. Chem. Res. 35, 2920–2928.

Manttari M., L. Puro, J. Nuortila-Jokinen & M. Nystrom, 2000. Fouling effects of polysaccharides and humic acid in nanofiltration, J. Membrane Sci. 165, 1–17.

Michel V., C. Marzin, G. Tarrago & J. Durand, 1998. New membranes bearing pyridinic ligands by plasma graft polymerization, J. Appl. Polym. Sci. 70, 359–366.

Minear R.A. & G.L. Amy, 1996. Disinfection By-products in Water Treatment: The Chemistry of Their Formation and Control. Lewis Publishers.

Nabe A., E. Staude & G. Belfort, 1997. Surface modification of polysulfone ultrafiltration membranes and fouling by BSA solutions, J. Membrane Sci. 133, 57–72.

Nilson J.A. & F.A. DiGiano, 1996. Influence of NOM composition on nanofiltration, J. AWWA 88, 53–66.

Patil A.V., R.C. Jain & R.A. Vora, 2001. Synthesis and characterization of graft copolymers of acrylic acid onto poly vinyl chloride using di-(2-phenoxy ethyl) peroxy dicarbonate initiator, Sci. Pure Appl. Chem. A 38, 681–698.

Pieracci J., J.V. Crivello & G. Belfort, 1999. Photochemical modification of 10 kDa polyethersulfone ultrafiltration membranes for reduction of biofouling, J. Membrane Sci. 156, 223–240.

Pieracci J., D.W. Wood, J.V. Crivello & G. Belfort, 2000. UV-assisted graft polymerization of N-vinyl-2-pyrrolidinone onto poly(ether sulfone) ultrafiltration membranes: Comparison of dip versus immersion modification techniques, Chem. Mat. 12, 2123–2133.

Pieracci J., J.V. Crivello & G. Belfort, 2002a. UV-assisted graft polymerization of N-vinyl-2-pyrrolidinone onto poly(ether

sulfone) ultrafiltration membranes using selective UV wavelengths, Chem. Mat. 14, 256–265.

Pieracci J., J.V. Crivello & G. Belfort, 2002b. Increasing membrane permeability of UV-modified poly(ether sulfone) ultrafiltration membranes, J. Membrane Sci. 202, 1–16.

Potts D.E., R.C. Ahlert & S.S. Wang, 1981. Critical limitations of fouling of reverse osmosis membranes, Desalination 36, 235–264.

Rautenbach R., T. Linn & D.M.K. Al-Gobaisi, 1997. Present and future pretreatment concepts – strategies for reliable and low-maintenance reverse osmosis seawater desalination, Desalination 110, 97–106.

Reid P.M., A.E. Wilkinson, E. Tipping & M.N. Jones, 1990. Determination of molecular weights of humic substances by analytical (UV scanning) ultracentrifugation, Geochim. Cosmochim. Acta 54, 131–138.

Saito N. & S. Yamashita, 1998. Characterization of surface-charge-mosaic-modified ultrafiltration membranes prepared by laser-induced surface graft polymerization, J. Appl. Polym. Sci. 67, 1141–1149.

Schafer A.I., A.G. Fane & T.D. Waite, 1998. Nanofiltration of natural organic matter: removal, fouling and the influence of multivalent ions, Desalination 118, 109–122.

Schulten H.R. & M. Schnitzer, 1993. A state of the art structural concept for humic substances, Naturwissenschaften 80, 29–30.

Sigal G.B., M. Mrksich & G.M. Whitesides, 1998. Effect of surface wettability on the adsorption of proteins and detergents, J. Am. Chem. Soc. 120, 3464–3473.

Symons J.M., T.A. Bellar, J.K. Carswell, J. DeMarco, K.L. Kropp, G.G. Robek, D.R. Seeger, C.J. Slocum, B.L. Smith & A.A. Stevens, 1975. National organics reconnaissance survey for halogenated organics, J. AWWA 11, 634–647.

Taniguchi M., J.E. Kilduff & G. Belfort, 2003a. Low fouling synthetic membranes by UV-assisted graft polymerization: monomer selection to mitigate fouling by natural organic matter, J. Membrane Sci. 222, 59–70.

Taniguchi M., J. Pieracci, W.A. Samsonoff & G. Belfort, 2003b. UV-assisted graft polymerization of synthetic membranes: mechanistic studies, Chem. Mat. 15, 3805–3812.

Taniguchi M., J.E. Kilduff & G. Belfort, 2003c. Modes of natural organic matter fouling during ultrafiltration, Environ. Sci. Technol. 37, 1676–1683.

Taniguchi M. & G. Belfort, 2004. Low protein fouling synthetic membranes by UV-assisted surface grafting modification: varying monomer type, J. Membrane Sci. 231, 147–157.

Thurman E.M., 1985. Organic Geochemistry of Natural Waters. Dordrecht, The Netherlands: Martinus Nijhofff/ Junk Publishers.

Thurman E.M. & R.L. Malcolm, 1981. Preparative isolation of aquatic humic substances, Environ. Sci. Technol. 15, 463–466.

Thurman E.M., R.L. Wershaw, R.L. Malcolm & D.J. Pinckney, 1982. Molecular size of aquatic humic substances, Org. Geochem. 4, 27–35.

Ulbricht M. & G. Belfort, 1995. Surface modification of ultrafiltration membranes by low-temperature plasma.

I. Treatment of polyacrylonitrile, J. Appl. Polym. Sci. 56, 325–343.

Ulbricht M. & G. Belfort, 1996. Surface modification of ultrafiltration membranes by low temperature plasma. II. Graft polymerization onto polyacrylonitrile and polysulfone, J. Membrane Sci. 111, 193–215.

Ulbricht M., H. Matuschewski, A. Oechel & H.-G. Hicke, 1996. Photo-induced graft polymerization surface modifications for the preparation of hydrophilic and low-protein-adsorbing ultrafiltration membranes, J. Membrane Sci. 115, 31–47.

Ulbricht M., K. Richau & H. Kamusewitz, 1998. Chemically and morphologically defined ultrafiltration membrane surfaces prepared by heterogeneous photo-initiated graft polymerization, Colloids Surf. 138, 353–366.

Van Reenen A.J. & R.D. Sanderson, 2002. Dynamically formed hydrous zirconium (IV) oxide-polyelectrolyte membranes. VII. Poly(acrylic acid-co-vinyl acetate) and poly(acrylic acid-co-vinyl alcohol) membranes. The effect of feed salt concentration on membrane properties, Desalination 85, 247–262.

Visvanathan C., B.D. Marsono & B. Basu, 1998. Removal of THMFP by nanofiltration: effects of interference parameters, Water Res. 32, 3527–3538.

Wang Y., J.-H. Kim, K.-H. Choo, Y.-S. Lee & C.-H. Lee, 2000. Hydrophilic modification of polypropylene microfiltration membranes by ozone-induced graft polymerization, J. Membrane Sci. 169, 269–276.

Wavhal D.S. & E.R. Fisher, 2002. Hydrophilic modification of polyethersulfone membranes by low temperature plasma-induced graft polymerization, J. Membrane Sci. 209, 255–269.

Xu Z., J. Wang, L. Shen, D. Men & Y. Xu, 2002. Microporous polypropylene hollow fiber membrane Part I. Surface modification by the graft polymerization of acrylic acid, J. Membrane Sci. 196, 221–229.

Yamagishi H., J.V. Crivello & G. Belfort, 1995a. Development of a novel photochemical technique for modifying poly(arylsulfone) ultrafiltration membranes, J. Membrane Sci. 105, 237–247.

Yamagishi H., J.V. Crivello & G. Belfort, 1995b. Evaluation of photochemically modified poly(arylsulfone) ultrafiltration membranes, J. Membrane Sci. 105, 249–259.

Yamaguchi T., T. Suzuki, T. Kai & S.-I. Nakao, 2001. Hollow-fiber-type pore-filling membranes made by plasma-graft polymerization for the removal of chlorinated organics from water, J. Membrane Sci. 194, 217–228.

Yoon S.-H., C.-H. Lee, K.-J. Kim & A.G. Fane, 1998. Effect of calcium ion on the fouling of nanofilter by humic acid in drinking water production, Water Res. 32, 2180–2186.

Yuan W. & A.L. Zydney, 1999a. Effects of solution environment on humic acid fouling during microfiltration, Desalination 122, 63–76.

Yuan W. & A.L. Zydney, 1999b. Humic acid fouling during microfiltration, J. Membrane Sci. 157, 1–12.

Yuan W. & A.L. Zydney, 2000. Humic acid fouling during ultrafiltration, Environ. Sci. Technol. 34, 5043–5050.

Zeeman A. & A.L. Zydney, 1996. Microfiltration and Ultrafiltration: Principles and Applications. New York: Marcel Dekker Inc.